Journal of
Materials Chemistry

Cite this: *J. Mater. Chem.*, 2011, **21**, 18317

www.rsc.org/materials

PAPER

Fabrication of electrochemically responsive surface relief diffraction gratings based on a multifunctional polyamide containing oligoaniline and azo groups†

Xiaoteng Jia,[a] Danming Chao,*[ab] Erik B. Berda,[b] Songhao Pei,[c] Hongtao Liu,[a] Tian Zheng[a] and Ce Wang*[a]

Received 18th August 2011, Accepted 14th September 2011
DOI: 10.1039/c1jm14047g

A novel, well-defined multifunctional polyamide bearing pendent aniline tetramer groups has been synthesized *via* low temperature solution polycondensation. The simultaneous presence of these two functional groups allows the polyamide to display the properties of azo-chromophore and oligoaniline, such as photoinduced birefringence and reversible electroactivity. The electrochromic performance of the polyamide shows the optical change in absorptivity depends on the various redox states of oligoaniline upon electrochemical switching. It is well known that a change in absorptivity is accompanied by a concomitant change in refractive index. By taking advantage of this effect and using the single step fabrication of surface relief gratings based on azo-chromophore, we have fabricated optical diffraction gratings with which the diffraction efficiency can be modulated by an electrochemical signal. Although patterned electroactive films have been made by many techniques, the copolymer approach employing the simple one-step surface relief gratings process displays optimal properties with respect to modulation depth and convenience, which avoids complicated electropolymerization steps or photochemical reactions. The electrochemically-induced modulation in the diffraction efficiency of the polyamide is believed to arise primarily from the effect of the redox state on the film's refractive index.

Introduction

During the past few years, electroactive polymers have gained exposure from their widespread applications in organic field-effect transistors, photovoltaic cells, light emitting diodes, and sensors.[1–4] The patterning of an electroactive or conductive polymer is often needed in the fabrication of microelectronic or -photonic devices[5] or microsensor arrays,[6] which have promising applications in microelectromechanical systems (MEMS), biosensors, cell-growth regulation, and microfluidic systems.[7–9] Diffraction gratings of electroactive polymer thin films are increasingly used as signal transduction layers in the sensing of NADH,[10] pH,[11] *etc*, attributed to the fact that the diffraction efficiency (DE) can be modulated with an electrochemical or chemical stimulus because of their reversible redox properties. To date, patterned surfaces are normally produced by toilful and sophisticated lithographic techniques or direct photochemical patterning.[12,13] Despite the success of these approaches in producing electroactive polymer periodic arrays,[14,15] most of these techniques either necessitate complex steps or modified electrodes in electrochemical polymerization, which would hamper the applications of the conducting polymer pattern films.

Azobenzene functionalized polymers have been intensively investigated for their photoresponsive properties and potential applications in diffractive optical elements, information storage, optical switching, sensors, and actuators.[16,17] On the basis of the optically induced *trans–cis* isomerization, azo-chromophore undergoes a macroscopic alignment to the direction of light polarization. In particular, the surface relief gratings (SRGs) formation observed for azo-polymer films, which is related to the mass transport process, is induced by exposure to the appropriate optical pattern.[18] This facile, erasable, single-step process allows quick fabrication of large or small area gratings having small periods, with good control over the grating parameters. Large amplitude SRGs in thin films of azo polymers with diverse chemical structures have been successfully written and the intriguing properties of the gratings continue to be reported.[19,20] As the electroactive group is readily covalently linked to the azo-polymer backbones, the multifunctional copolymers with photoinduced mass-transport properties can be developed this way. However, this approach has not yet been extended for fabricating diffractive gratings in films of multifunctional azo-copolymers with pendent electroactive groups.

---

[a] *Alan G. MacDiarmid Institute, College of Chemistry, Jilin University, Changchun, 130012, P.R. China. E-mail: chaodanming@jlu.edu.cn; cwang@jlu.edu.cn; Fax: +86-431-85168292; Tel: +86-431-85168292*
[b] *Department of Chemistry and Materials Science Program, University of New Hampshire, Durham, NH, 03824, USA*
[c] *College of Physics, Jilin University, Changchun, 130012, P. R. China*

† Electronic supplementary information (ESI) available. See DOI: 10.1039/c1jm14047g

As model compounds of polyaniline (PANI), monodispersed oligoanilines with well-defined structures have been heavily investigated due to their good electroactivity, enhanced solubility and excellent processability.[21,22] Recently, considerable effort has been made in chemically synthesizing polymers based on oligoanilines, such as graft, alternating, and star-like polymers.[23–25] The introduction of pendent oligoaniline groups into azo-polymer backbones is quite promising as the properties of the multifunctional copolymers can be tuned reversibly *via* electrochemical modification or light irradiation. As to the pure azo-polymers, the SRGs can be easily formed in thin films but the DE of the grafting can't be modulated with an electrochemical stimulus, because the azo group has no electroactivity. Similarly, pure polyaniline can only exhibit the electrochromic property and can't be prepared to a patterned film by itself. In this regard, copolymerization of azo-chromophore and oligoaniline allows for the single step photofabrication of optical diffraction gratings based on the azo group and gives rise to a modification of DE supplied by reversible redox states of oligoaniline responding to electrochemical modulation. To the best of our knowledge, research about the formation of electrochemically responsive SRGs based on electroactive azo polymers is still lacking in the literature.

We report herein a novel multifunctional polyamide (Azo-PA-S-AT) with pendent aniline tetramer groups synthesized *via* low temperature solution polycondensation. The electrochromic properties, photo-orientation process and the stable value of birefringence are presented in detail. We also describe the preparation of photoinduced SRGs based on the film of Azo-PA-S-AT and investigated the DE of the fabricated gratings responding to the electrochemical modulation.

Results and discussion

Characterization and basic properties of Azo-PA-S-AT

The one-step synthetic route for the electroactive diamine monomer (EDA) is shown in Scheme S1.† The preparation of EDA was carried out by K_2CO_3-mediated nucleophilic reaction and toluene was used to dehydrate the reaction system. The reaction temperature was first controlled at 140 °C to remove the water generated during the phenoxide formation, and then increased slowly to 160 °C to accomplish the reaction. The multifunctional polyamide with pendant oligoaniline group in Scheme 1 was prepared by low temperature solution polycondensation. The chemical structure of Azo-PA-S-AT was confirmed by FTIR, ^{1}H NMR spectroscopy and GPC. An FTIR spectrum of the polyamide showed the characteristic absorption bonds around 3380 cm^{-1} corresponding to N–H stretching vibration, around 2923 cm^{-1} based on C–H stretching vibration in methyl groups and around 1658 cm^{-1} due to C=O stretching vibration in aryl carbonyl groups. The bond around 1452 cm^{-1} was attributed to the stretching vibration of N=N and the peak at 1205 cm^{-1} could be assigned to the stretching vibration of C–O–C of the aryl ether linkages. The ^{1}H NMR stacked spectrum of Azo-PA-S-AT is shown in Fig. S1.† The protons located at the electron-rich *ortho*-ether position were strongly shielded, and their signals appeared at high-field region (7.34–6.62 ppm), while the protons located at *para*- or *ortho*-positions of carbonyl groups were deshielded due to their strongly electron-withdrawing effects, and their signals appeared at low-field region (8.05–7.85 ppm). The number-average molecular weight (M_n) of Azo-PA-S-AT was found to be 3.30 × 10^4 with a polydispersity index (M_w/M_n) of 1.62.

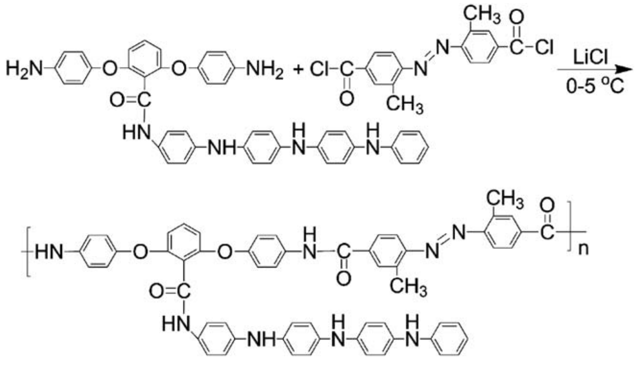

Scheme 1 The synthetic route of the multifunctional polyamide (Azo-PA-S-AT).

The polyamide exhibited outstanding solubility in polar solvents such as NMP, DMF and DMAc, and the enhanced solubility could be attributed to the attachment of bulky pendent groups. Thus, the excellent solubility makes the polymer a potential candidate for practical applications in spin or dip-coating processes. The crystallization of Azo-PA-S-AT was investigated by wide-angle X-ray diffraction pattern and the result indicates that the polyamide was essentially amorphous, revealing that the introduction of bulky pendant aniline tetramer groups disturbed the close packing and regularity of the polymer chains. The thermal properties of Azo-PA-S-AT were evaluated by differential scanning calorimetry (DSC) and thermogravimetric analysis (TGA). In the DSC curve, the polyamide showed no clear melting endotherms up to the decomposition temperatures, indicating the amorphous nature of the polyamide. The glass transition temperature (T_g) of the polyamide was found to be 158 °C. The TGA trace for this material displayed only a single step weight loss indicative of backbone decomposition. The temperature for 10% weight loss of polyamide in nitrogen was 418 °C. The char yield of polyamide at 700 °C in nitrogen was 61 wt%.

Electrochemical activity

The electrochemical behavior of Azo-PA-S-AT was investigated by cyclic voltammetry (CV) and the results were shown in Fig. 1. A DMAc solution of the polyamide was cast on the g-c working electrode and evaporated to form a thin solid film. The CV of the electrode was performed in 1 mol L^{-1} H_2SO_4 at different potential scan rates (20–140 mV s^{-1}). The CV of the electrode underwent two oxidation processes with the oxidation peaks at 370 and 530 mV. The first oxidation peak corresponded to the transition of leucoemeraldine base (LEB)/emeraldine base (EB), and the second peak corresponded to the transition of emeraldine base (EB)/pernigraniline base (PNB). A linear dependence of the peak currents as a function of scan rates in the region of 20–140 mV s^{-1} (inset of Fig. 1) confirmed both a surface controlled process[26] and a well-adhered electroactive polymer

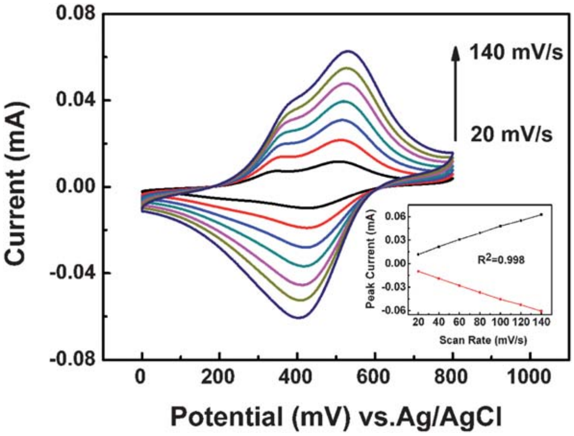

Fig. 1 CV of the Azo-PA-S-AT electrode in 1mol L^{-1} H_2SO_4 at different potential scan rates: 20–140 mV s^{-1}. The inset shows the relationships between the oxidation peaks and reduction current *vs.* potential scan rate.

film. The Azo-PA-S-AT film was found to be very stable with almost no change in its CV diagram after 50 repeated cyclic scans between 0 and 0.8 V.

Spectroelectrochemistry and electrochromic performances

The electro-optical properties of Azo-PA-S-AT film were investigated using the changes in absorption spectra under a voltage pulse. Spectroelectrochemical studies were performed on the film of polyamide spin-coated on an Indium-Tin Oxide (ITO) glass slide in 0.01 mol L^{-1} H_2SO_4 couple at applied potentials of −0.2, 0, 0.2, 0.4, 0.6 and 0.8 V (*vs.* Ag/AgCl). Fig. 2 presented the UV-Vis absorption spectra of the polyamide film at various applied potentials. The peak at 425 nm (related to polarons of oligoaniline) increased gradually as the potential increased from −0.2 to 0.4 V. With an increase in applied potential beyond 0.4 V, the peak decreased as a broad band associated with superimposed contributions of polaronic and bipolaronic species of oligoaniline at ~800 nm was introduced.[26] The color of the polyamide thin films changed from a transmissive yellowish (at −0.2 V), to green (at *ca.* 0.4 V), and finally to an absorptive brown blue (at *ca.* 0.8 V) (inset of Fig. 2). The above results indicated that it could be a highly effective method for producing multicolor electrochromic materials using different concentrations of the two chromophores through copolycondensation.

Electrochromic switching studies were carried out to monitor changes in the optical contrast at 700 nm during repeated potential stepping between the neutral (−0.2 V) and oxidized state at 0.8 V with a residence time of 60 s. The results for the first 5 cycles were shown in Fig. 3. The optical contrast value (%ΔT) was found to be 32% at 700 nm measured between its coloring (oxidization) and bleaching (reduction) states. Switching time was the time required to bring the polyamide to its most reduced state from its most oxidized state or *vice versa*. It was defined as the time required for reaching 90% of the full change in the coloring/bleaching process. The polyamide revealed a switching time of 2.7 s at 0.8 V for the coloring process at 700 nm and 1.8 s for bleaching. The coloration efficiency CE ($\eta = \Delta OD/Q$) was a practical tool to measure the power requirements of an electrochromic material. It was measured by monitoring the amount of ejected charge (Q) as a function of the change in optical density (ΔOD) of the polymer film. The electrochromic behavior of the polyamide exhibited CE up to 128.7 cm^2 C^{-1} (at 700 nm) at the first oxidation stage.

Photoisomerization of Azo-PA-S-AT

Photoisomerization studies were carried out by irradiating the DMAc solution and spin-coated thin film, respectively. As shown in Fig. 4(a), the UV-Vis absorption spectra revealed an absorption band centered around 333 nm, which was associated with the overlap of the π–π* transition of the benzoid rings of oligoaniline and the azobenzene moiety.[27] As the irradiation time increased, the intensity of the absorption decreased and the absorption band underwent a blue shift, due to a *trans*-to-*cis* photoisomerization process of the azobenzene chromophore. The blue shift might be induced by the decrease in the extent of π-conjugation due to the photoisomerization.[28] On the other

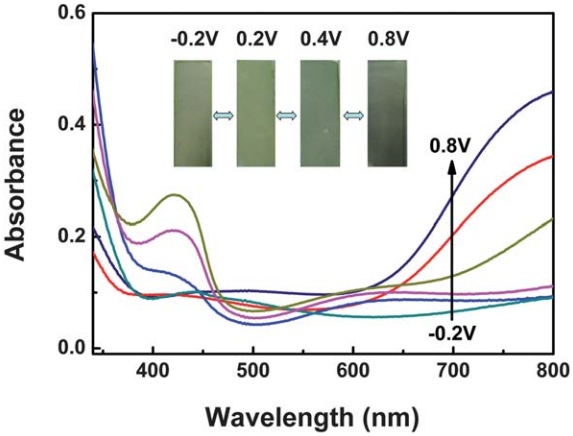

Fig. 2 The spectral changes of an Azo-PA-S-AT/ITO electrode (0.6 × 3 cm^2) in 0.01 mol L^{-1} H_2SO_4 at different potentials. The inset shows photographs of the Azo-PA-S-AT/ITO electrode at different potentials.

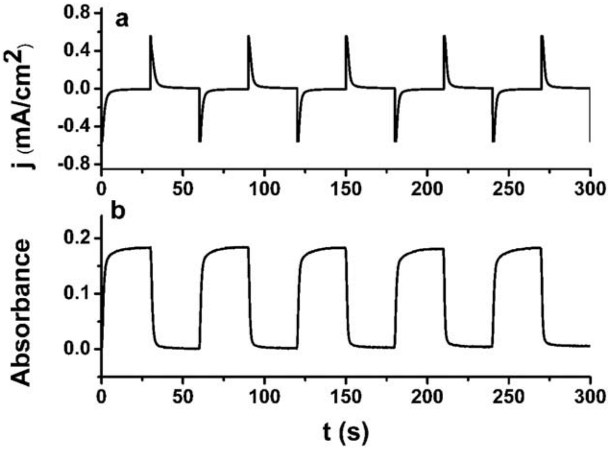

Fig. 3 (a) Current consumption and (b) absorbance changes monitored at 700 nm of an Azo-PA-S-AT/ITO electrode in 0.01mol L^{-1} H_2SO_4 for the first 5 cycles.

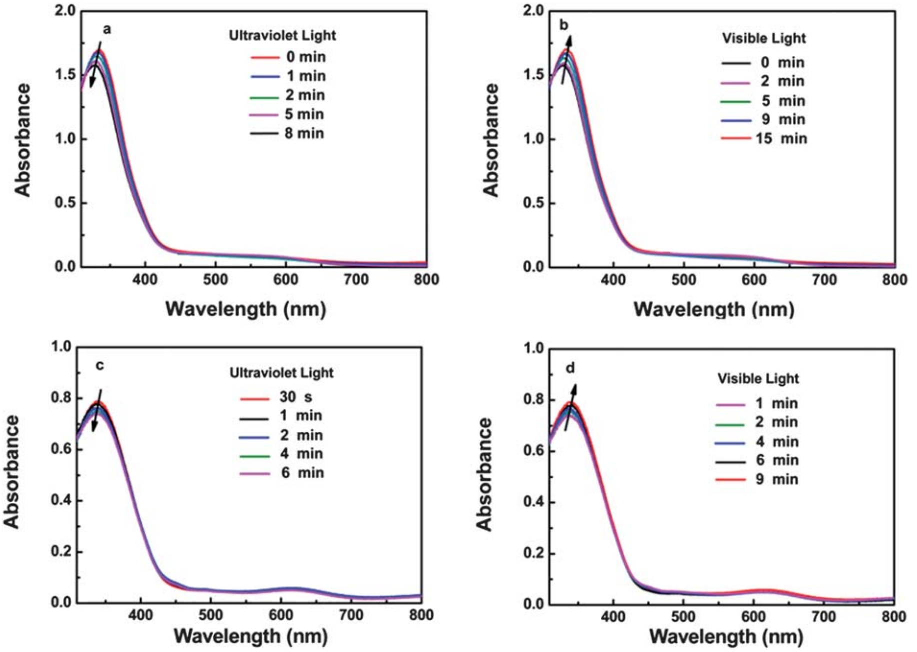

Fig. 4 Changes in the UV-Vis absorption spectra of Azo-PA-S-AT with different irradiation times: (a) and (b) in DMAc solution, (c) and (d) as spin-coated films.

hand, when the solution was irradiated with visible light, the absorption peak at 333 nm (Fig. 4(b)) will gradually recover to its initial value prior to irradiation. We also conducted this process on a spin-coated thin film, and the results in Fig. 4(c) and (d) exhibited a similar reversibility to those in solution. Compared with the spectra of the polyamide in DMAc solution, the λ_{max} for the thin film red-shifted to 340 nm, which might be caused by a solvatochromic effect of the azo chromophores.[29] Besides, the time to reach a photostationary state for the solid film was shorter than that in solution. It was related to the relative lower concentration of the polymer in the film.

Photoinduced birefringence

Optical storage experiments were carried out using a pump beam (532 nm of Nd:YAG laser) with a polarization angle of 45° with respect to the polarization direction of a low-power laser operating at 850 nm (reading beam). The wavelength of the probe light was just outside the absorption band of the film of Azo-PA-S-AT in LEB form. The experimental set-up was similar to that previously reported.[30]

A typical multiple writing–erasing curve of the polyamide film was presented in Fig. 5. Before irradiation, no optical anisotropy was observed because of the random orientation of the azo chromophore. As the polarized Nd:YAG laser beam radiation was introduced (point A), an anisotropic orientation distribution was expected immediately as a consequence of the alignment of the azo chromophore changing on account of the *trans–cis–trans* isomerization of the azo moiety. While the writing beam was turned off at point B, the birefringence value exhibited a little decay and then reached a stable state in a few minutes. It was mainly caused by thermally activated dipole reorientation which would tend towards randomization of the anisotropy.[31] Compared with other azo-polymers,[32,33] the birefringence conserved after relaxation declined a little with the remaining birefringence larger than 96% of the initial value, indicating that the polyamide presented improved stability in the case of the photoinduced orientation. This was mainly attributed to the high glass transition temperature and rigid aromatic structure of the polyamide which limited the relaxation process of the oriented chromophore groups.[34] Finally, the azo-chromophore orientation was completely randomized after circularly polarized light was introduced (point C). Moreover, the maximum and saturated value of the photo-induced birefringence changed slightly after several cycles.

Patterning of Azo-PA-S-AT thin films

In past years, lots of work has focused on approaches to produce micropatterned films of electroactive polymers.[35,36] However,

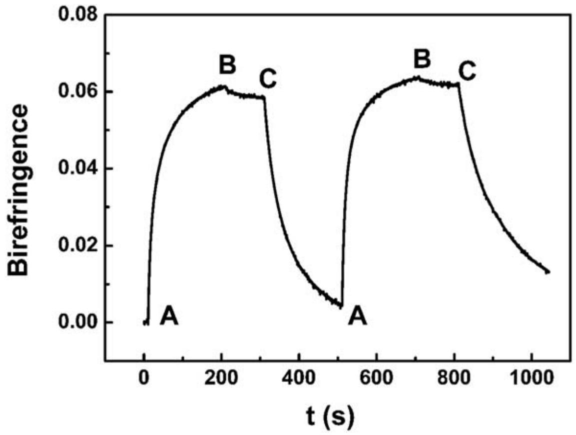

Fig. 5 Multiple 'writing–erasing' photoinduced birefringence on Azo-PA-S-AT film ($d = 4$ μm) at room temperature.

multistep photolithographic techniques and electropolymerization steps are commonly required for the fabrication of patterned electroactive polymer films. Recently, the developed photofabrication process of surface relief gratings (SRGs) has offered for a quick formation of diffraction gratings with desired periods.[37] On the other hand, oligoaniline with well-defined structure shows reversible redox properties during the electrochemical switching. So we can take advantages of single step photofabrication of patterned films based on the azo group and various redox states of oligoainile responding to electrochemical modulation to prepare electrochemically responsive diffraction gratings.

A typical experimental setup used for the photofabrication of SRGs has been reported.[19] Exposing Azo-PA-S-AT film to two interfering linearly p-polarized beams (Nd:YAG laser, 355 nm) formed the surface-relief gratings. It is a good way to increase storage capacity using a shorter wavelength of light as demonstrated by the new BluRay technology. SRGs of the polyamide could be rapidly fabricated within 20 s at room temperature at an intensity of 80 mW cm^{-2}. After forming the SRGs, the exposed region is scanned with an Atomic Force Microscope (AFM, Nanoscope III, Digital Instruments) in tapping mode. Fig. 6 showed a representative region of the surface of patterned film. The gratings revealed a well-shaped micropattern with an amplitude modulation of 147 nm. The spatial period was equal to the period of the interference pattern of 1.4 μm, depending on both the angle between the two interfering beams and the wavelength of the writing beam.

Electrochemically modulated optical diffraction gratings

The diffraction efficiency (DE) of a grating depends on the optical properties (the absorptivity k and the refractive index n) of a grating material.[38] It is well-known that oligoaniline exhibits a change in absorptivity (k) concomitant with a change in redox state during electrochemical switching due to the electrochromic effect. At the same time, the refractive index (n) of oligoaniline will also change with the redox states due to the close relationship between the absorptivity (k) and the refractive index (n) according to the Kramers–Kronig relation.[39] By making use of this effect and employing the SRGs formation process described above, we have fabricated optical diffraction gratings with which the DE can be modulated by an electrochemical signal.

The apparatus used for DE measurements is similar to the previous literature.[40] The experimental example of the electrochemical modulation of the DE for the grating-patterned polyamide film was shown in Fig. 7. The SRGs were supported on an ITO electrode and subjected to potential cycling (−0.2 to 1.0 V), while the intensities of the transmitted and first-order diffracted beams from a 633 nm He–Ne laser were monitored. As can be seen, these electrochemically-induced changes in DE could be reversibly switched many times, and the signal was lagging behind the potential variation. Between −0.2 and 0.2 V, the DE remained constant when the polyamide was reduced to the LEB form. Interestingly, as the potential increased from 0.2 to 0.7 V, the DE decreased while the polyamide gratings changed from LEB to EB, then to PNB. With the potential increased beyond 0.7 V, the DE changed slightly because the polyamide was totally oxidized to the PNB form without any influence on its structure. This was in accordance with the change of n of polyaniline following the potential variation,[41,42] as the DE was considerably more sensitive to changes in n than to changes in absorptivity.[43] The origin of the redox-induced modulation in the DE was predominated by the change of n, which was coupled with the oligoaniline oxidation/reduction. In addition, the signal lagging behind the potential variation is about 25 s. However, the hysteresis was not observed in the spectroelectrochemical measurements. This phenomenon could be explained possibly as follows. First of all, during the SRG formation process, the photoinduced alignment of polymer chains and large-scale

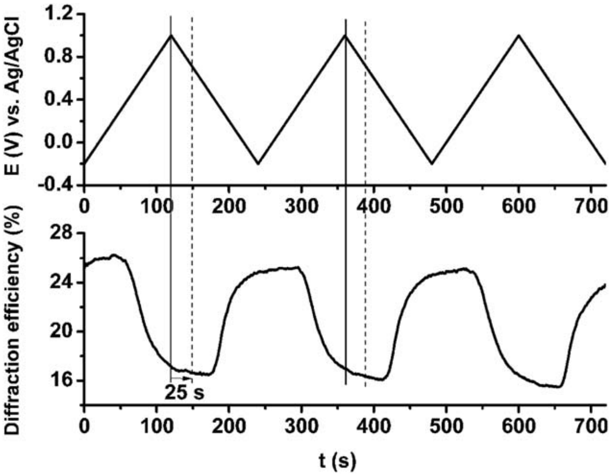

Fig. 7 Diffraction efficiency changes with the potential change of Azo-PA-S-AT diffraction gratings at a sweep rate of 10 mV s^{-1}.

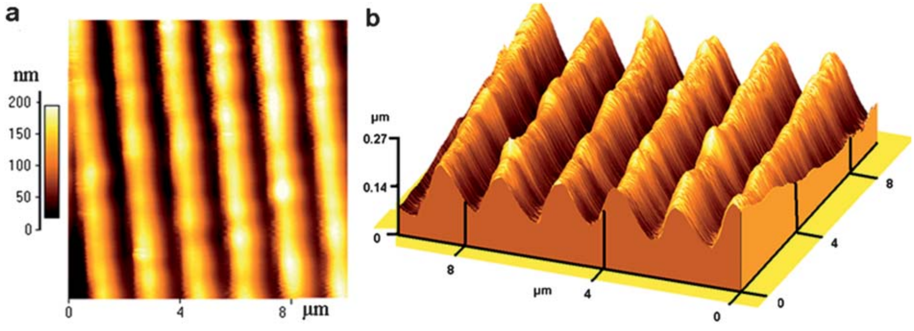

Fig. 6 AFM images of a patterned Azo-PA-S-AT film, (a) the plane view of the SRGs (10 × 10 μm^2), (b) a typical 3-D view of the SRGs.

macromolecular motion lead to a change in the microstructure of the films. Consequently, the conductivity of the film will also change, which gives rise to an obvious hysteresis. Another contributory factor is the much thicker thickness of the film for SRGs. As a result, it will spend more time completing the exchange of the neutral molecular and ion between the solution and the film, which is an essential process of redox cycling.

Conclusions

Well-defined oligoaniline-containing azo-polyamide prepared by low temperature solution polycondensation exhibits high T_g, good thermal stability and reversible electrochemical properties. The obtained polyamide reveals valuable electrochromic characteristics with a high contrast value, low switching times and moderate coloration efficiency. The polyamide presents high stability of the induced order (96% of photoinduced birefringence is maintained after relaxation) upon irradiation. Utilization of the one-step photofabrication of SRGs as electrochemically responsive diffraction gratings was demonstrated. This single step approach offers an opportunity to fabricate patterns in electroactive azo polymer films. The electrochemically induced changes in diffraction efficiency are in accord with the change in the refractive index that occurs concomitant with a change in the redox state of the oligoaniline. This multifunctional polyamide, bearing distinct functional groups, will be of potential interest, since it is suitable for smart windows, optical switches, reversible high density optical storage and diffraction-based sensing devices.

Experimental

Materials

All chemicals, including 3-methyl-4-nitrobenzoic acid, sodium hydroxide, glucose, acetic acid, thionyl chloride, 4-aminophenol and anhydrous lithium chloride, were purchased from Shanghai Chemical Factory. DMAc and toluene were used as received without further purification. Distilled water was self-made. Anhydrous potassium carbonate was dried at 110 °C for 24 h before use. Optically transparent ITO glass substrates (Reintech electronic technologies CO., 10 Ω/square) with dimensions of 6.0×0.6 cm^2 were used as thin film electrodes.

Measurements

Mass spectrometry (MS) was performed on an AXIMA-CFR laser desorption ionization time of flight spectrometer (COMPACT). Fourier-transform infrared spectra (FTIR) measurements were recorded on a BRUKER VECTOR 22 spectrometer. The nuclear magnetic resonance spectra (NMR) were run on a BRUKER-500 spectrometer. The number-average molecular weight (M_n), weight-average molecular weight (M_w), and molecular weight distribution of the polymer were measured with a gel permeation chromatography (GPC) instrument equipped with a Shimadzu GPC-802D gel column and SPD-M10AVP detector with DMF as an eluent at a flow rate of 1 mL min^{-1}. Wide-angle X-ray diffraction (WAXD) measurements were made using a Siemens D5005 diffractometer equipped with a Cu-Kα radiation source at room temperature. Differential scanning calorimeter (DSC) measurements were performed on a Mettler Toledo DSC821^e instrument. A Perkin-Elmer PYRIS 1 TGA was used to investigate the thermal stability of the polymer. The CV was investigated on a CHI 660c Electrochemical Workstation (CH Instruments, USA) with a conventional three-electrode cell, using an Ag/AgCl cell as the reference electrode, a platinum wire electrode as the counter electrode, and a glassy carbon electrode (Φ3.0 mm) as the working electrode. Spectroelectrochemical measurements were carried out in a cell built from a 1 cm commercial cuvette using a UV-2501 PC Spectrometer (SHIMADZU). The ITO-coated glass was used as the working electrode, a Pt wire as the counter electrode, an Ag/AgCl cell as the reference electrode and 0.01 mol L^{-1} H_2SO_4 as the electrolyte. Photoisomerization of Azo-PA-S-AT was conducted using a high pressure mercury lamp in conjunction with a band-pass UV filter (λ_{max} = 360 nm). UV-Vis spectra were recorded on a UV-2501 PC Spectrometer.

Synthesis of electroactive diamine monomer (EDA)

The synthetic routes for the preparations of compound 1 and EDA are depicted in Scheme S1.† We have reported the suitable preparation of EDA in the literature.[44]

MALDI-TOF-MS: *m/z* calculated for $C_{43}H_{36}N_6O_3$ = 684.78. Found 685.0. FTIR (KBr, cm^{-1}): 3380 (s, υ_{NH}), 3037 (m, υ_{CH}), 1657 (*vs*, $\upsilon_{C=O}$), 1602 (s, $\upsilon_{C=C}$ of benzenoid rings), 1506 (*vs*, $\upsilon_{C=C}$ of benzenoid rings), 1294 (s, υ_{C-N}), 1233 (m, υ_{C-O-C}), 829 (m, δ_{CH}), 750 (m, δ_{CH}), 696 (m, δ_{CH}). ^{1}H NMR (d_6-DMSO, ppm): δ = 10.24 (s, 1H, due to H_1), δ = 7.74 (s, 1H, due to H_4), δ = 7.69 (s, 1H, due to H_3), δ = 7.60 (s, 1H, due to H_2), δ = 7.54 (d, 2H, due to H_7), δ = 7.14 (t, 3H, due to H_6, H_9), δ = 6.93 (d, 12H, due to H_{10}), δ = 6.81 (d, 4H, due to H_{13}), δ = 6.67 (t, 1H, due to H_5), δ = 6.59 (d, 4H, due to H_{12}), δ = 6.29 (d, 2H, due to H_8), δ = 4.99 (s, 4H, due to H_{11}).

Synthesis of *trans*-azobenzene-4,4′-dicarbonyl chloride (compound 3)

12 g 3-menthyl-4-nitrobenzoic acid (66.2 mmol) and sodium hydroxide (40 g, 1 mol) were dissolved in 250 mL water and the solution was kept at 50 °C. A solution of glucose (80 g, 444 mmol) in 120 mL water was added dropwise in 40 min to the above solution with stirring at 50 °C. The reaction was maintained at 50 °C in the air for 16 h. After cooling down to room temperature, the mixture was adjusted to pH 6 with glacial acetic acid and the precipitate was collected by filtration. Then it was purified by recrystallization with hot K_2CO_3 solution.

2.98 g compound 2 (10 mmol), 60 mL thionyl chloride, and few drops of DMF were combined in a flask at 90 °C for 10 h. Thionyl chloride was removed from the solution by simple distillation. The residue was purified by reduced pressure distillation to afford *trans*-azobenzene-4,4′-dicarbonyl chloride 2.64 g (yield: 88%).

MALDI-TOF-MS: *m/z* calculated for $C_{16}H_{12}Cl_2N_2O_2$ = 335.18. Found 335. FTIR (KBr, cm^{-1}): 3081 (m, υ_{C-H} of benzenoid rings), 2972 (m, υ_{C-H} of methyl groups), 1763 (*vs*, $\upsilon_{C=O}$), 1747 (s, $\upsilon_{C=O}$), 1593 (m, $\upsilon_{C=C}$ of benzenoid rings), 1421 (m, $\upsilon_{N=N}$), 822 (m, δ_{CH}), 760 (w, δ_{CH}), 686 (m, δ_{CH}). ^{1}H NMR

($CDCl_3$, ppm): $\delta = 8.13$ (s, 2H, due to H_d), $\delta = 8.02$ (dd, 2H, due to H_a), $\delta = 7.66$ (d, 2H, due to H_b), $\delta = 2.81$ (s, 6H, due to H_c).

Synthesis of the multifunctional polyamide (Azo-PA-S-AT)

A solution of 2.738 g (4 mmol) EDA in 30 mL DMAc was added dropwise over a period of 2 h to a stirred mixture of compound 3 (1.2735 g, 3.8 mmol) and anhydrous lithium chloride (0.3545 g, 6 mmol) in 100 mL DMAc. The reaction was carried out in an ice bath with a nitrogen flow. Following the addition of the solution of EDA, the resulting mixture was stirred for 4 h and then poured into water. The product, filtered from the mixture, was subsequently washed with water three times and acetone once, filtered and dried in a vacuum oven at 50 °C for 24 h. The brown powder was obtained in 87% yield.

FTIR (KBr, cm^{-1}): 3380(m, υ_{NH}), 3029 (w, $\upsilon_{C–H}$ of benzenoid rings), 2923 (m, $\upsilon_{C–H}$ of methyl groups), 2854 (w, $\upsilon_{C–H}$ of methyl groups), 1658 (m, $\upsilon_{C=O}$), 1602(s, $\upsilon_{C=C}$ of benzenoid rings), 1504 (vs, $\upsilon_{C=C}$ of benzenoid rings), 1452 (m, $\upsilon_{N=N}$), 1301 (s, $\upsilon_{C–N}$), 1205 (m, $\upsilon_{C–O–C}$), 821 (m, δ_{CH}), 748 (m, δ_{CH}), 696 (m, δ_{CH}). ^1H NMR (d_6-DMSO, ppm): $\delta = 10.44$ (due to H_1), $\delta = 10.34$ (due to H_2), $\delta = 8.05–7.85$ (due to $H_{13–15}$), $\delta = 7.70–7.53$ (due to $H_{3–5}$), $\delta = 7.34–6.62$ (due to $H_{6–12}$), $\delta = 2.78$ (due to H_{16}). GPC: number-average molecular weight (M_n) 3.30×10^4; polydispersity (M_w/M_n) 1.62.

Preparation of polymer films

Azo-PA-S-AT was dissolved in DMAc (10 wt%) and then filtered with a mesh filter with 0.45 μm pore. Amorphous thin films were obtained by spin coating (for spectroelectrochemical measurements, photoisomerisation process and SRGs) or casting (for birefringence) the polymer solution onto ITO substrates, which were cleaned in an ultrasonic bath with DMF, ethanol and distilled water subsequently. The thickness of the films were controlled to be about 0.5–1.0 μm for fabricating SRGs and 2–8 μm for the photoinduced birefringence experiment. The residual solvent was removed by heating the films in a vacuum oven at 60 °C for 12 h.

Optical arrangement

The birefringence measurement was produced with a Nd:YAG pump laser beam (532 nm) polarized at 45° with respect to the probe beam polarization. The photoinduced birefringence (Δn) was determined according to $\Delta n = \lambda/\pi d \times \sin^{-1} (I/I_0)^{1/2}$, where λ is the wavelength of the reading beam, d is the film thickness, I is the intensity of the reading beam after the second polarizer and I_0 is the transmitted intensity of the reading beam between parallel polarizers in the absence of anisotropy.

Films spin coated on ITO glass were illuminated by two coherent beams from a p-polarized Nd:YAG laser beam (Spectra-Physics, Quanta-Ray-150, 355 nm) with an equal intensity of 80 mW cm^{-2}, where the laser beam was split by beam splitting (BS) and the reflected half-beam coincided with the other half on the film surface. Laser intensities given in this report were measured just after the collimating lens. The gratings were characterized by the depth and shape of the surface modulation by AFM (Nanoscope III, Digital Instruments, tapping mode). Electrochemical diffraction modulation was performed in a quartz cuvette using a CHI 660c Electrochemical Workstation, with a Pt wire used as the counter electrode, an Ag/AgCl cell as the reference electrode and 0.01 mol L^{-1} H_2SO_4 as the electrolyte. To characterize a grating, a probe beam of He–Ne laser beam (632.8 nm) was passed through an aperture that made the beam diameter adjustable and then perpendicularly irradiated on the grating. The zero-order and first-order diffraction beams were collected with silicon photodiodes which are fixed on the optical stages for fine adjustment of the positions. The DE of the gratings was calculated as the ratio of I_1/I_0, where I_0 and I_1 were the intensities of incident light and light in the 1st diffraction order, respectively.

Acknowledgements

This work has been supported in part by the National Natural Science Foundation of China (No. 21104024 and 50973038), and the National 973 Project (No. S2009061009).

Notes and references

1 A. Pron, P. Gawrys, M. Zagorska, D. Djurado and R. Demadrille, *Chem. Soc. Rev.*, 2010, **39**, 2577–2632.
2 Y. J. Cheng, S. H. Yang and C. S. Hsu, *Chem. Rev.*, 2009, **109**, 5868–5923.
3 Q. Wang and D. G. Ma, *Chem. Soc. Rev.*, 2010, **39**, 2387–2398.
4 C. Li, H. Bai and G. Q. Shi, *Chem. Soc. Rev.*, 2009, **38**, 2397–2409.
5 R. M. Leasure, J. A. Moss and T. J. Meyer, *Inorg. Chem.*, 1994, **33**, 1247–1248.
6 M. L. Renak, G. C. Bazan and D. Roitman, *Adv. Mater.*, 1997, **9**, 392–395.
7 M. Geissler and Y. Xia, *Adv. Mater.*, 2004, **16**, 1249–1269.
8 C. H. Alarcon, T. Farhan, V. L. Osborne, W. T. S. Huck and C. Alexander, *J. Mater. Chem.*, 2005, **15**, 2089–2094.
9 J. M. Razal, M. Kita, A. F. Quigley, E. Kennedy, S. E. Moulton, R. M. I. Kapsa, G. M. Clark and G. G. Wallace, *Adv. Funct. Mater.*, 2009, **19**, 3381–3388.
10 S. J. Tian, N. R. Armstrong and W. Knoll, *Langmuir*, 2005, **21**, 4656–4660.
11 P. N. Bartlett and E. Simon, *Phys. Chem. Chem. Phys.*, 2000, **2**, 2599–2606.
12 T. Chen, D. P. Chang and S. Zauscher, *Small*, 2010, **6**, 1504–1508.
13 K. S. Schanze, T. S. Bergstedt and B. T. Hauser, *Adv. Mater.*, 1996, **8**, 531–534.
14 F. S. Marikkar, C. Carter, K. Kieltyka, J. W. F. Robertson, C. Williamson, A. Simmonds, R. Zangmeister, T. Fritz and N. R. Armstrong, *Langmuir*, 2007, **23**, 10395–10402.
15 M. C. Tria, J. Y. Park and R. Advincula, *Chem. Commun.*, 2011, **47**, 2393–2395.
16 A. Natansohn and P. Rochon, *Chem. Rev.*, 2002, **102**, 4139–4176.
17 N. K. Viswanathan, D. Y. Kim, S. P. Bian, J. Williams, W. Liu, L. Li, L. Samuelson, J. Kumar and S. K. Tripathy, *J. Mater. Chem.*, 1999, **9**, 1941–1955.
18 A. S. Matharu, S. Jeeva, P. R. Huddleston and P. S. Ramanujam, *J. Mater. Chem.*, 2007, **17**, 4477–4482.
19 L. Andruzzi, A. Altomare, F. Ciardelli, R. Solaro, S. Hvilsted and P. S. Ramanujam, *Macromolecules*, 1999, **32**, 448–454.
20 D. R. Wang, G. Ye, X. L. Wang and X. G. Wang, *Adv. Mater.*, 2011, **23**, 1122–1125.
21 D. M. Chao, X. F. Lu, J. Y. Chen, X. G. Zhao, L. F. Wang, W. J. Zhang and Y. Wei, *J. Polym. Sci., Part A: Polym. Chem.*, 2006, **44**, 477–482.
22 R. A. Singer, J. P. Sadighi and S. L. Buchwald, *J. Am. Chem. Soc.*, 1998, **120**, 213–214.
23 K. Buga, R. Pokrop, A. Majkowska, M. Zagorska, J. Planes, F. Genoud and A. Pron, *J. Mater. Chem.*, 2006, **16**, 2150–2164.
24 D. M. Chao, X. F. Lu, J. Y. Chen, X. C. Liu, W. J. Zhang and Y. Wei, *Polymer*, 2006, **47**, 2643–2648.
25 B. L. Guo, W. A. Finne and A. C. Albertsson, *Macromolecules*, 2010, **43**, 4472–4480.

26 M. Malta, E. R. Gonzalez and R. M. Torresi, *Polymer*, 2002, **43**, 5895–5901.
27 S. C. Yang, R. J. Cushman and D. Zhang, *Synth. Met.*, 1989, **29**, 401–408.
28 E. M. Genies, A. Boyle, M. Lapkowski and C. Tsintavis, *Synth. Met.*, 1990, **36**, 139–182.
29 P. C. Che, Y. N. He and X. G. Wang, *Macromolecules*, 2005, **38**, 8657–8663.
30 X. B. Chen, Y. H. Zhang, B. J. Liu, J. J. Zhang, H. Wang, W. Y. Zhang, Q. D. Chen, S. H. Pei and Z. H. Jiang, *J. Mater. Chem.*, 2008, **18**, 5019–5026.
31 A. Natansohn, P. Rochon, M. Pézolet, P. Audet, D. Brown and S. To, *Macromolecules*, 1994, **27**, 2580–2585.
32 S. Wu, S. Y. Duan, Z. Y. Lei, W. Su, Z. S. Zhang, K. Y. Wang and Q. J. Zhang, *J. Mater. Chem.*, 2010, **20**, 5202–5209.
33 S. W. Cha and D. H. Choi, *Adv. Funct. Mater.*, 2001, **11**, 355–360.
34 C. Cojocariu and P. Rochon, *J. Mater. Chem.*, 2004, **14**, 2909–2916.
35 M. H. Jung and H. Lee, *Langmuir*, 2008, **24**, 9825–9831.
36 S. Holdcroft, *Adv. Mater.*, 2001, **13**, 1753–1765.
37 E. Ishow, B. Lebon, Y. N. He, X. G. Wang, L. Bouteiller, L. Galmiche and K. Nakatani, *Chem. Mater.*, 2006, **18**, 1261–1267.
38 B. T. Hauser, T. S. Bergstedt and K. S. Schanze, *J. Chem. Soc., Chem. Commun.*, 1995, (19), 1945–1946.
39 S. Gottesfeld, *Electroanal. Chem.*, 1989, **15**, 143–265.
40 A. M. Massari, K. J. Stevenson and J. T. Hupp, *J. Electroanal. Chem.*, 2001, **500**, 185–191.
41 A. Baba, S. J. Tian, F. Stefani, C. J. Xia, Z. H. Wang, R. C. Advincula, D. Johannsmann and W. Knoll, *J. Electroanal. Chem.*, 2004, **562**, 95–103.
42 D. R. Kim, W. Cha and W. K. Paik, *Synth. Met.*, 1997, **84**, 759–760.
43 K. S. Schanze, T. S. Bergstedt, B. T. Hauser and C. S. P. Cavalaheiro, *Langmuir*, 2000, **16**, 795–810.
44 X. T. Jia, D. M. Chao, H. T. Liu, L. B. He, T. Zheng, X. J. Bian and C. Wang, *Polym. Chem.*, 2011, **2**, 1300–1306.